Iğdır Üniversitesi Fen Bilimleri Enstitüsü Dergisi, 12(3): 1529 - 1538, 2022
Journal of the Institute of Science and Technology, 12(3): 1529 - 1538, 2022

ISSN: 2146-0574, eISSN: 2536-4618

Physics **DOI: 10.21597/jist.1091686**

Research Article

Received: 22.03.2022 **Accepted: 15.06.2022**

To Cite: Hacıismailoğlu M, 2022. Structural and Magnetic Properties of Electrodeposited Cobalt-Polypyrrole Composite Films. Journal of the Institute of Science and Technology, 12(3): 1529 - 1538.

Structural and Magnetic Properties of Electrodeposited Cobalt-Polypyrrole Composite Films

Mürşide HACIİSMAİLOĞLU [1*]

ABSTRACT: Co particles were electrodeposited at an electrode potential of -2.0 V on ITO/PPy (500 nm) substrates. During Co electrodeposition, charge density was changed from 400 to 5000 mC cm^{-2} in order to control the Co amount. Current density-time transients showed that the dominant reaction is PPy undoping for the initial times and Co deposition for the later times. Structural characterization was done by a Fourier transformed infrared (FTIR) spectrometer and a scanning electron microscope (SEM). FTIR spectra of the Co-PPy composite films have similar to that of the PPy film but peak intensities decrease as the charge density increases due to the surface covering by Co (by SEM). The chemical composition was detected by an energy dispersive spectrometer. For all films, C and N (belonging to PPy layer), O (due to oxidized character of PPy layer), F (doping anion) and Co peaks were obtained. Magnetic properties were measured by a vibrating sample magnetometer. Some films with Co charge density of 600, 700, 4000 and 5000 mC cm^{-2} have nearly isotropic magnetic behavior and the others are anisotropic. The isotropic behavior may arise from the very weak texture and preferred orientation of the films.

Keywords: Co particles, magnetic materials, polypyrrole, composite materials, VSM

[1] Mürşide HACIİSMAİLOĞLU (**Orcid ID:** 0000-0001-5648-3230), Bursa Uludag University, Faculty of Arts and Sciences, Department of Physics, Görükle, Bursa, Türkiye

***Corresponding Author:** Mürşide HACIİSMAİLOĞLU, e-mail: msafak@uludag.edu.tr

INTRODUCTION

Composite materials produced from conductive polymers incorporating metal particles attract much attention due to the wide range of application areas. So far, they have been studied as an electrocatalytic material because the catalytic activity of a composite material containing Pt and Pd for hydrogen and methanol oxidation, and oxygen reduction are higher than that of the metal (Vork et al., 1986, Vassar et al., 1988, Tian et al. 2009). They are also efficiently used for gas sensing such as NH_3, H_2 and CO, and microwave absorbance (Torsi et al., 1998). Spin-OLEDs and nanoelectronic devices may be potential application areas for such composite materials.

Composite materials are commonly synthesized by chemical and electrochemical techniques. The electrochemical technique is a simple, rapid and cheap one. It allows changing physical and chemical parameters during the growth of polymer and metal particles, which conduces to produce a film having optimum properties and maximum functional yield. Most composite materials are prepared electrochemically in two stages, firstly conductive polymer is electropolymerized by doping ion on a conductive substrate, and then metal particles are electrodeposited on/in the polymer. In recent years, ferromagnetic metals (Co, Ni, Fe and alloys) are electrodeposited on/in conductive polymers to have composite materials (Haciismailoglu, 2015, Haciismailoglu et al., 2014, Zolopa et al., 2013, Ko et al. 2002, Orinakova and Filkusova, 2010, Heinig et al., 2008, Chowdhury et al., 2007, Chipara et al., 2007, Damian and Omanovic, 2006, Trung et al., 2005, Watanabe et al., 2004, Hepel et al., 1996, Lee and Tan, 1990). These metals cause conductive polymers to gain magnetic behavior and there is very limited study on their magnetic properties. Conducting ferromagnetic polymer materials can be employed for magnetic semiconductors, data storage devices, electric or magnetic shielding and microwave absorbing (Garcia et al. 2002, McNally et al. 2005). Chowdury et. al. (Chowdhury et al., 2007) investigated the interaction between polyaniline (PANI) and Ni, and studied on magnetic and conductive properties of the composite materials. The magnetic susceptibility measurements of PANI-Ni were showed that Ni supplies a ferromagnetic behavior to the PANI. Watanabe et. al. (Watanabe et al., 2004) had research on the electronic, structural and magnetic properties of Co-PPy composite materials. It was reported that there is an interaction between PPy and Co, and those Co particles impart a magnetic behavior to the composite materials. In our previous paper on Co-PPy composite materials, it was obtained that the magnetic anisotropy is affected by PPy film thickness, and the magnetic moment increases depending on increasing Co charge density (Haciismailoglu, 2015, Haciismailoglu et al., 2014). Chipara et. al. (Chipara et al., 2007) produced Fe- PPy films by changing the deposition potential and the electrolyte concentration. It was found that as the deposition potential increases both coercivity and magnetic anisotropy of the films increase. Ko et. al. (Ko et al. 2002) prepared composite materials containing PPy and ferromagnetic metal alloys (NiFe and CoMnP). The composite materials with NiFe and CoMnP alloys showed soft and hard magnetic behaviors respectively.

The deposition potential of the ferromagnetic metal is in the same range as the reduction potential of the conductive polymers, which affects the deposition process of the ferromagnetic metals. Therefore, at this potential range, the polymer reduction and the metal deposition must be evaluated together. Moreover, since the conductivity of a polymer is not as much as that of a metal, an ohmic potential drop occurs and it causes decreasing the overpotential as the potential becomes more negative (Tsakova, 2008). Despite these disadvantages, it was reported that the conductive polymer can supply a current efficiency higher than a metal substrate by inhibiting the hydrogen evolution (Hepel et al., 1996). Besides, due to its fibril structure, it presents a deposition area larger than a metal substrate

(Hepel et al., 1996, Lee and Tan, 1990). The aim of this article is to investigate the effects of Co amount on the magnetic behavior of Co-PPy composite materials and evaluate electrochemical, chemical, structural properties together. From the results, the deposition parameters can be determined for the composite materials adapted to the potential application areas.

MATERIALS AND METHODS

The required chemical materials of acetonitrile, pyrrole, tetrabutylammonium hexafluorophosphate ($TBA{\cdot}PF_6$), cobalt sulfate ($CoSO_4{\cdot}7H_2O$) were bought from Sigma–Aldrich and employed as received. The pyrrole was kept at 4°C before use. The ultrapure water of Elga Felix system (resistivity = 18.2 M) was used for all experiments.

The composite films were produced potentiosatically in two stages in a three electrode cell. Firstly, the PPy layers were electropolymerized on indium tin oxide (ITO) substrates from a Py solution containing 0.1 M pyrrole, 0.5 M $TBA{\cdot}PF_6$ and acetonitrile. A Pt sheet and a saturated calomel electrode (SCE) were counter and reference electrodes respectively. Before the electropolymerization the ITO substrates were ultrasonically cleaned in ethanol and acetone, and then masked with a Kapton tape except deposition area. The PPy layer was deposited at the potential of 0.9 V vs SCE and the thickness was determined as 500 nm based on works done before (Haciismailoglu 2015). In the second stage, ITO/PPy layer was immersed in Co solution which contains 0.3 M $CoSO_4{\cdot}7H_2O$ in order to electrodeposit Co particles at a potential of -2.0 V vs. SCE. The charge density of the Co particles was changed from 400 to 5000 mC cm^{-2}. In order to obverse and compare the electrochemical and structural changes occurred on the PPy layer during Co deposition the PPy layer was reduced at the electrode potential of -2.0 V vs SCE in a solution having 0.3 M Na_2SO_4. The charge density was varied from 400 to 3000 mC cm^{-2}. These obtained films are reduced forms of PPy layer. Na_2SO_4 solution was chosen since it has SO_4^{2-} ions and almost the same pH value as the used Co solution.

For electrochemical characterization, during Co deposition, the current density-time transients on both ITO substrate, and PPy layer on ITO substrate (ITO/PPy) in Co solution were recorded. Also for comparison, the same was done in the Na_2SO_4 solution. The structural characterization of the PPy layer (oxidized form), reduced forms of PPy layer and Co-PPy composite films were studied by using a Fourier transformed infrared (FTIR) spectroscope. The transmittance was recorded as T% depending on wavenumber between 600 and 3500 cm^{-1}. The morphology of the composite films was investigated by a scanning electron microscope (SEM). The images were obtained at an accelerating voltage of 20.00 kV from a working distance of 11.0 mm with a magnification of 3000X. The chemical analysis was done by energy dispersive X-ray spectrometer (EDX) attached to the SEM. The measurements were made from the solution side of the composite films. The magnetic behavior was studied by a vibrating sample magnetometer (VSM). The magnetic field was applied parallel and perpendicular to the film plane. The magnetic moment of each sample was measured in the unit of emu. Then obtained values are divided to nominal Co mass calculated from Faraday law by assuming 100% current efficiency. In the plots, the magnetic moment was given as the magnetization in the unit of emu g^{-1}. The saturation magnetization (M_s), remnant magnetization (M_r), squareness ($S= M_s/ M_r$) and coercivity (H_c) values were determined from the hysteresis curves.

RESULTS AND DISCUSSION

Figure 1 shows current density-time transients of bare ITO and ITO/PPy layer in Na_2SO_4 and Co solution for the first 15 s. The inset figure (green curve) displays the whole part of the ITO/PPy layer in the Co solution, which represents the deposition of Co particles on the ITO/PPy layer to produce a

composite film. The red curve corresponds to the deposition of a Co film on an ITO substrate. The black and blue curves are the electrochemical response of the ITO substrate and ITO/PPy layer in Na_2SO_4 solution respectively, which were obtained to compare with the results measured in Co solution. For all of them, the applied electrode potential is -2.0 V vs SCE. At such a potential, three different reactions occur simultaneously which are PPy reduction (undoping), Co deposition and hydrogen evolution. As seen the initial current density is very low for Co particles deposited on ITO/PPy layer (the green curve) while for the Co film deposited on ITO is the highest. The low current value is due to the IR drop arising from the low conductivity of the PPy layer. Despite the difference in current value, the initial behavior of ITO/PPy layer in Co and Na_2SO_4 solution is similar. So it may be concluded that at the beginning PPy reduction is dominant but in Co solution the reduction is hindered by the Co ions and hence make the current lower. As seen from the inset figure as the time lasts the current density of Co particles keeps increasing up to 4 mA/cm^2. The current density increment arises from Co deposition dominantly. Those results are compatible with the EDX and VSM results. Magnetic measurements showed that a very low magnetic moment was detected for the composite film having Co at the charge density of 400 mC cm^{-2} for which short times needed. On the other hand, according to the EDX spectra, the peak belonging to F (due to PF_6^- doping ion) appeared for the composite film with Co grown at the charge density of as high as 5000 mC cm^{-2}. Those results prove that the competition lasts between Co deposition and PPy reduction throughout the entire experiment.

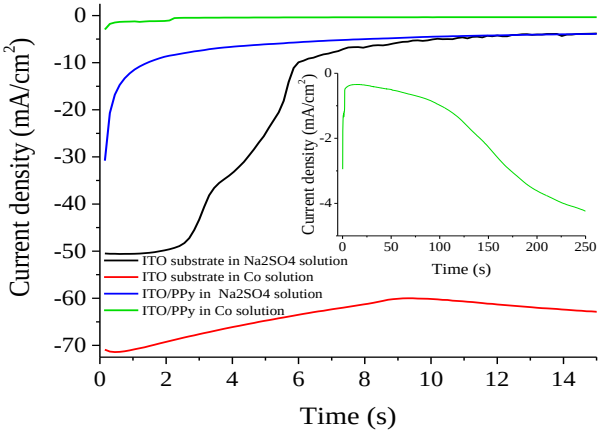

Figure 1. The current density-time transients of bare ITO substrate in Na_2SO_4 (black curve) and Co solutions (red curve), and of PPy/ITO in Na_2SO_4 (blue curve) and Co solutions (green curve).

Figure 2 shows FTIR spectra of the oxidized PPy film and its reduced forms at the charge density of 400, 600, 800, 1000 and 3000 mC cm^{-2} in Na_2SO_4 solution. Firstly, the characteristic peaks of the oxidized PPy film, which are very consistent with the results found in previous works (Tian and Zerbi, 1990, Davidson and Turner, 1995, Street et al., 1982, Lei et al. 1992) are evaluated. Then the slight changes for the reduced forms are mentioned. In the spectrum of the oxidized PPy film, the sloping baseline and undetectable N-H stretching band at around 3400 cm^{-1} are signs of fully oxidizing (Davidson and Turner, 1995). The peaks of 2966 and 2879 cm^{-1} represent asymmetrical and symmetrical C-H stretching respectively. The bands at 1540, 1476 and 1385 cm^{-1} are attributed to C-N, C-C and C=C stretching. The peak of 1164 cm^{-1} arises from C-C vibrations. The peaks positioned at 1035 and 934 cm^{-1} are due to C-H in plane and C-H out of plane bending vibrations respectively. The peaks at 882 and 836 cm^{-1} represent the ring bending of α-carbon atoms. The peak of 739 cm^{-1} arises from the ring bending of β-carbon atoms. The intensity of the peaks belonging to α-carbon atoms is

much more prominent than that of β-carbon atoms (Tian and Zerbi, 1990, Davidson and Turner, 1995, Street et al., 1982). For the reduced films, the sloping baseline is not observed, as a result of decreasing conductivity due to the reduction. However the detected peaks remain almost in the same position, but slight intensity changes and peak broadening are obtained. Also, some new peaks at around 1100, 1260 and 1607 cm^{-1}, representing N-H bonding, C-H bending and C=C out of plane bending vibrations respectively appeared as a result of reduction (Lei et al. 1992, Kato et al. 1991, Martins dos Santos et al. 2006).

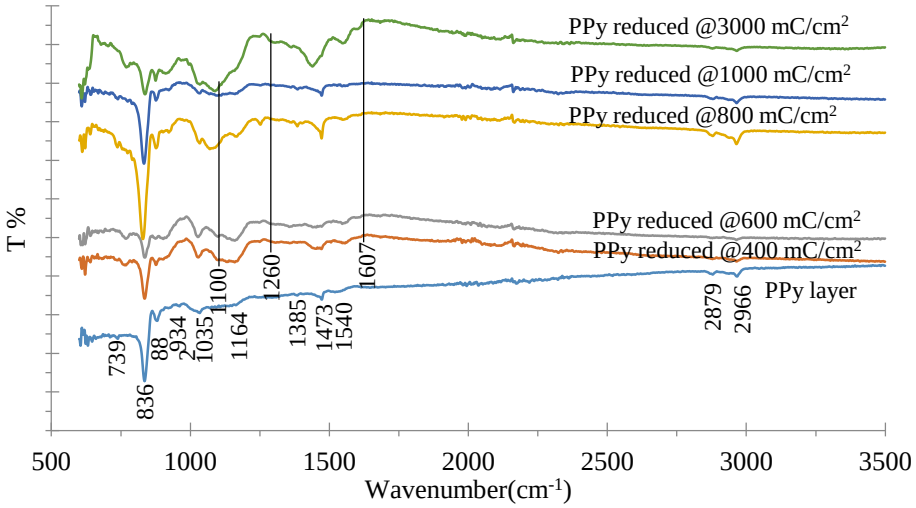

Figure 2. FTIR spectra of the oxidized PPy film, and of PPy films reduced at the charge density of 400, 600, 800, 1000 and 3000 mC cm^{-2}

Figure 3 represents FTIR spectra of the composite films with Co particles produced at the charge density of 800, 1000, 3000, 5000 mC cm^{-2}. The bands of the composite films are evaluated on the basis of the oxidized PPy film shown in Figure 2. The peaks seen at 739, 1035, 1164, 1385 and 1540 cm^{-1} disappeared. The intensity of the peaks positioned at 836, 882, 1476, 2879 and 2966 cm^{-1} decrease as Co charge density increases. These detected disappearing and intensity decreasing may arise from the Co particles covering all PPy surfaces as the Co charge density increases (by SEM). Obtaining the peaks at 882 and 836 cm^{-1} confirms that PPy films still preserve α-α bonding during Co deposition. Moreover, the peaks of 1476, 2879 and 2966 cm^{-1} reveal that it has enough conductivity to deposit Co particles. In the EDX spectra of the composite films, recording the peak of F for all shown charge densities supports this result. Besides, some new peaks are observed between 1035 and 1164 cm^{-1}, these are 1069 cm^{-1} (for 800 mC cm^{-2}), 1100 cm^{-1} (for 1000 and 3000 mC cm^{-2}) and 1125 cm^{-1} (for 5000 mC cm^{-2}) due to an interaction between N and Co atoms (Watanabe et al., 2004, Kato et al. 1991,Liu and Hwang, 1999). The peaks at 1294 and 1630 cm^{-1} are attributed to C-H bending and C=C wagging of the reduction of PPy which simultaneously occurs during Co deposition (Martins dos Santos et al. 2006).

Figure 4 displays the SEM images of the composite films with Co particles at the charge density of (a) 600, (b) 800, (c) 1000, (d) 3000 and (d) 5000 mC cm^{-2}. For 600 mC cm^{-2} charge density (Fig. 4a), Co particles start to grow all PPy surface but prefer to aggregate in some areas dendritically. In other areas, the film surface having small, white and circular Co particles (by EDX) was observed as shown in the inset figure (with 1000X magnification). For the charge density of 800 mC cm^{-2} (Fig. 4b), circular Co particles with different sizes appeared on the surface.

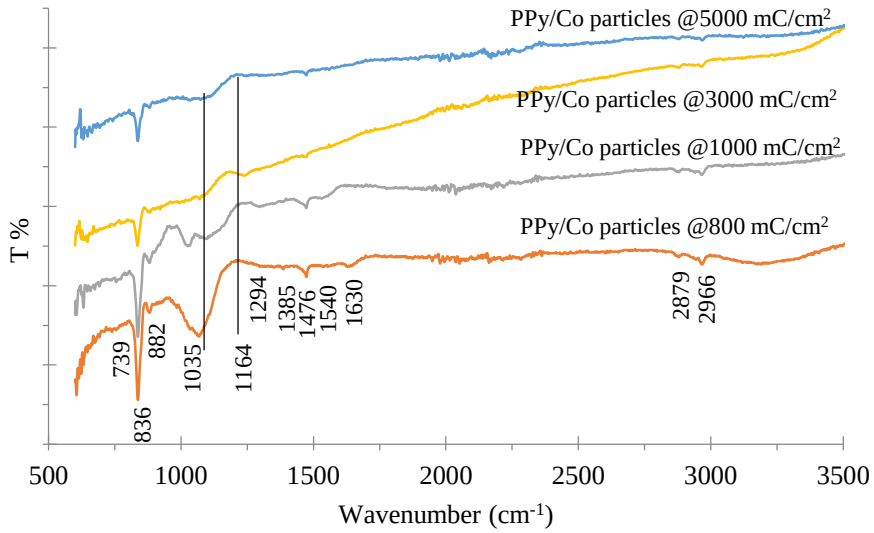

Figure 3. FTIR spectra of the Co-PPy composite films having Co particles with the charge density of 800, 1000, 3000 and 5000 mC cm^{-2}

The areas without circles have very less of Co (by EDX) and seem like a fibril structure. For 1000 mC cm^{-2} charge density (Fig. 4c), Co spread to the entire surface even at the curves of the PPy film. This may be the beginning of the continuous film tendency. As seen from Fig. 4d and e the films having Co particles with the charge density of 3000 and 5000 mC cm^{-2} have similar surfaces. The size of Co particles gets bigger as the charge density increases. Even for 5000 mC cm^{-2} charge density, Co particles contact to each other and become almost like a thin film. This result is consistent with the FTIR spectra in which it was recorded that the intensity of the peaks decreases as the charge density increases.

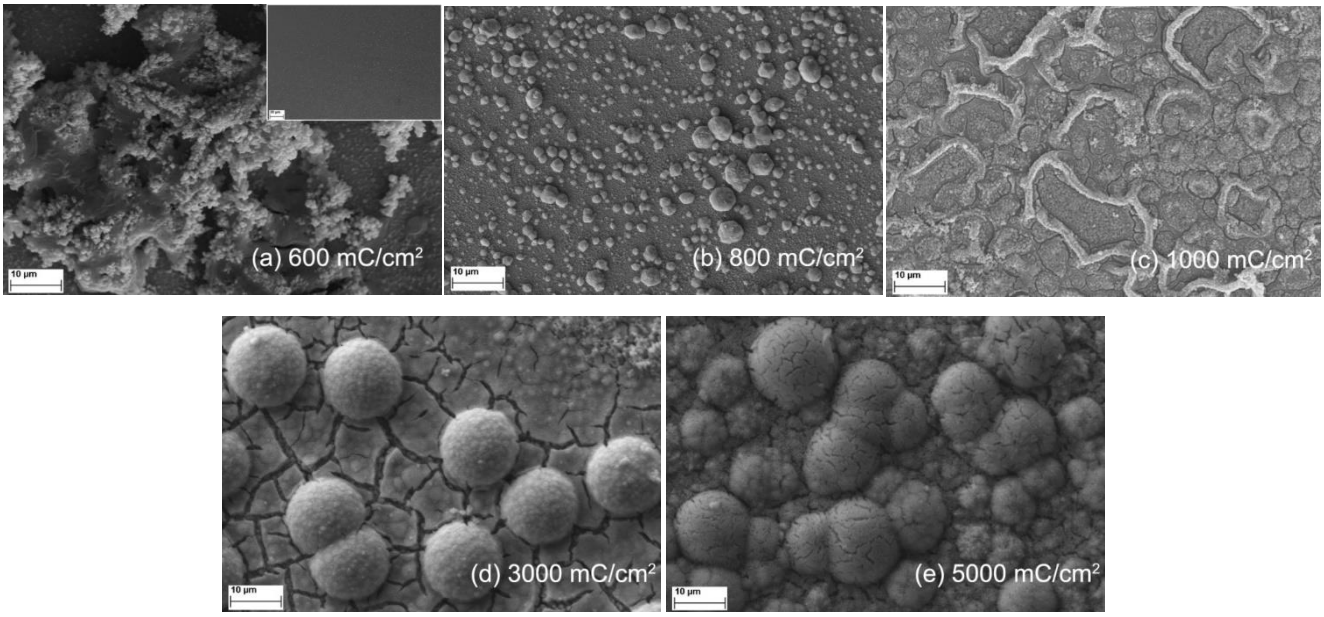

Figure 4. SEM images of the composite films with Co particles at the charge density of (a) 600, (b) 800, (c) 1000, (d) 3000 and (e) 5000 mC cm^{-2}

Figure 5 represents EDX spectra of the composite films having Co particles with the charge density of 600, 800, 3000 and 5000 mC cm^{-2}. The spectrum for the composite film having Co with the charge density of 1000 mC cm-2 was presented in previous work (Haciismailoglu, 2015). A square measurement area was chosen for each film at 100X magnification. The peaks of Au and Pd arise from the top coating. The peaks of Si, In and Sn are due to ITO substrates. As the charge density increases

the intensity of ITO peaks decreases, except for 5000 mC cm^{-2}. C and N elements are marked as 1 and 2 respectively. The films have O, showing as 3, which is attributed to the oxidizing character of the PPy layer. The peak belonging to the F element of the doping anion (PF_6^-) appears and is labeled as 4, but the peak of P is not observed because of overlapping with the Au peak at around 2.1 keV. Detecting the F element proves that the PPy layer still contains doping anion even at a charge density as high as 5000 mC cm^{-2}. The K_α (6.9 keV) and L_α (0.78 keV) peaks of Co are very clear for each film and their intensity increases as the Co charge density increases. For the film having Co with the charge density of 5000 mC cm^{-2}, the intensity of these peaks decreases and of substrate peaks increases. For high Co charge density, during cleaning the composite film, some of the Co particles adhering loosely on the surface are removed. This result reflects to the magnetic measurements.

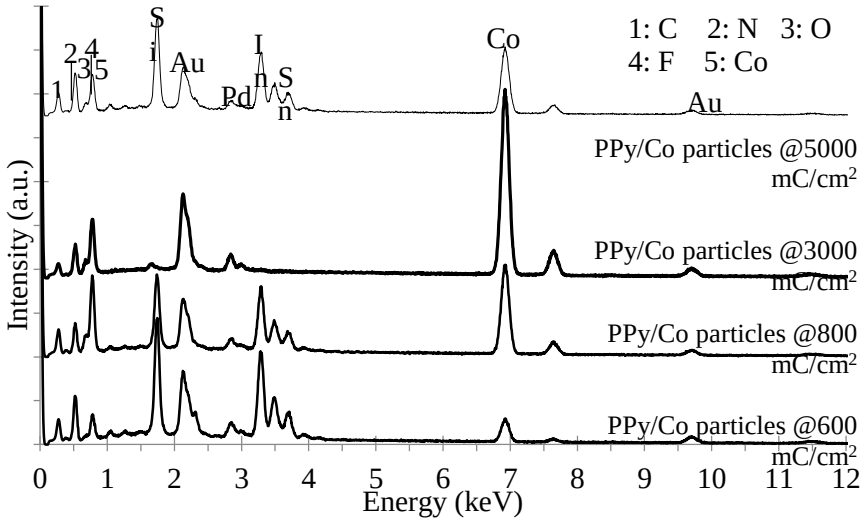

Figure 5. EDX spectra of the composite films having Co particles at the charge density of (a) 600, (b) 800, (c) 1000, (d) 3000 and (e) 5000 mC cm^{-2}

Fig. 6 displays two examples of the hysteresis curves of the Co-PPy composite films having Co particles deposited at (a) 600 and (b) 3000 mC cm^{-2} charge density for which magnetic field applied parallel (blue line) and perpendicular (red line) to the film plane. As seen, the films have different magnetic behavior against the applied magnetic field. For 600 mC cm^{-2} charge density, the parallel and perpendicular magnetizations show almost the same magnetic field dependence namely it has nearly isotropic behavior. For the charge density of 700, 4000 and 5000 mC cm^{-2} the films have similar behavior. For 3000 mC cm^{-2} charge density, the magnetization saturates at a parallel magnetic field lower than that of the perpendicular one. So that, it has anisotropic behavior and the easy axis is in the film plane. Similar curves were obtained at the charge density of 800, 1000 and 2000 mC cm^{-2} as well. The hysteresis curves are related to the microstructure of the composite films. This isotropic property arises from very weak crystal texture and preferred orientation of Co-PPy composite films (Haciismailoglu, 2015). Such isotropic hysteresis curves are also obtained for nanowires and thin films, having very weak preferred orientation (Kaur et al., 2013, Cao et al., 2013, Iannotti et al., 2008). Fig 6c shows hysteresis curves for the films produced at all studied charge densities. The composite films having Co particles with the charge density of 400 and 500 mC cm^{-2} have a diamagnetic effect dominantly. For the charge density more than 500 mC cm^{-2}, the films show a ferromagnetic behavior that increases as a function of the charge density up to 1000 mC cm^{-2}. Also for those films, the magnetization value decreases at high magnetic fields due to the diamagnetic effect of the PPy layers. For higher charge densities, the magnetic moment values fluctuate as a result of removed Co particles during cleaning after electrodeposition which is consistent with the EDX results. Saturation

magnetization (M_s), remnant magnetization (M_r), squareness (S) and coercivity (H_c) values for the cases of parallel and perpendicular applied magnetic field are given in Table 1.

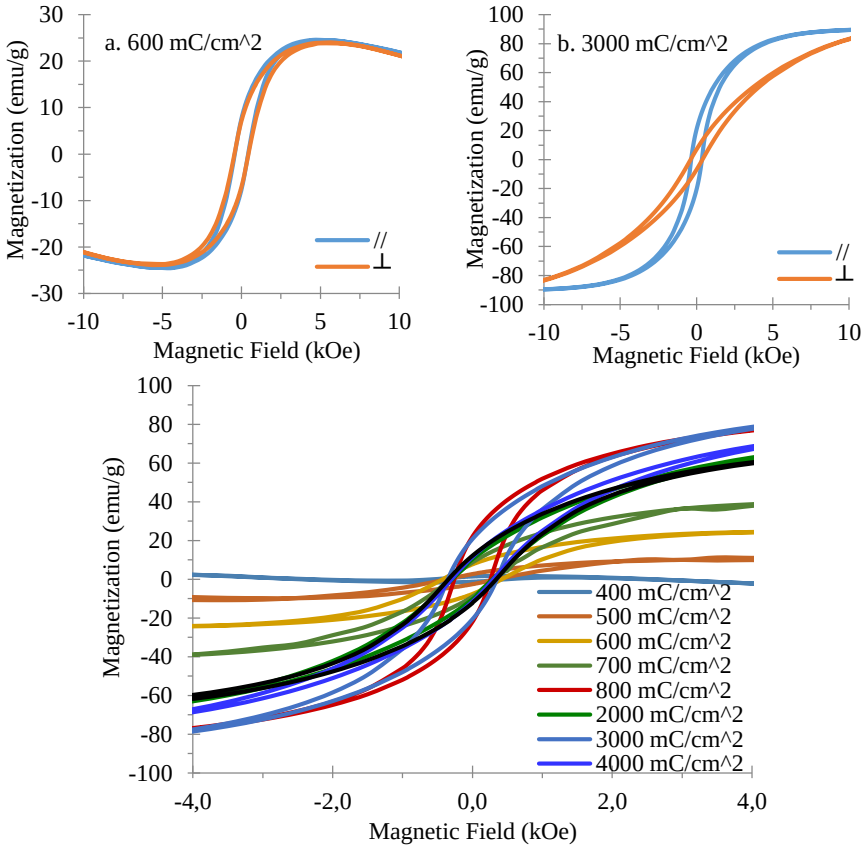

Figure 6. The hysteresis curves of the Co-PPy composite films having Co particles at the charge density of (a) 600 and (b) 3000 mC cm^{-2}, and (c) the hysteresis curves of all studied charge densities

Table 1. Saturation magnetization, remnant magnetization, squareness and coercivity values for the case of parallel and perpendicular applied magnetic field

Charge density (mC cm^{-2})	Magnetic behavior	Parallel				Perpendicular			
		M_s (emu g^{-1})	M_r (emu g^{-1})	S	H_c (Oe)	M_s (emu g^{-1})	M_r (emu g^{-1})	S	H_c (Oe)
400				Diamagnetic					
500				Diamagnetic					
600	isotropic	24.53	7.648	0.312	423.0	23.93	7.118	0.297	444.0
700	isotropic	40.64	8.839	0.217	319.5	39.27	6.958	0.177	330.3
800	anisotropic	108.2	13.63	0.126	237.0	113.1	5.157	0.046	302.0
1000	anisotropic	Ref. 5	Ref. 5	Ref. 5	Ref. 5	Ref. 5	Ref. 5	Ref. 5	Ref. 5
2000	anisotropic	74.71	10.37	0.139	288.4	58.30	3.921	0.067	255.8
3000	anisotropic	90.58	20.69	0.228	351.6	93.69	6.988	0.075	387.0
4000	isotropic	82.76	11.54	0.139	299.6	92.21	9.561	0.104	323.6
5000	isotropic	70.62	12.25	0.173	341.8	76.45	8.162	0.107	356.0

All M_s values are smaller than that of the value of bulk Co (162.5 emu g^{-1}) and M_r is not higher than 21 emu g^{-1}. The composite materials with Co at the charge density of 600 and 700 mC cm^{-2} have relatively low M_s values due to the small amount of Co (by EDX). Also, Co particles are not homogenous on the surface (Fig. 4a), so the magnetic interaction of the Co atoms will not be so strong which causes low M_s and M_r. The films having Co with a charge density more than 700 mC cm^{-2} possess high M_s and M_r values since Co starts growing all around the surface. The S values are interpreted by comparing the cases of parallel and perpendicular magnetic fields. Each film showing isotropic behavior has close S values for both cases, but the films with anisotropic behavior have different S values. All films are hard magnetic materials since their H_c values are higher than 125 Oe.

CONCLUSION

Co-PPy composite films were produced by electrochemically on ITO substrates as a function of Co charge density changed between 400 and 5000 mC cm^{-2}. For comparison, the current density-time transients of bare ITO and PPy (500 nm)/ITO substrates were recorded in Na_2SO_4 and Co solutions. It was concluded that once the potential is applied, PPy reduction and hydrogen evolution occur dominantly, and then Co deposition is taken place more. PPy film, showing characteristic bands by FTIR, has enough conductivity to deposit Co on itself. For the composite films, the intensity and position of some peaks change, and some new peaks appear due to an interaction between Co and N atoms. SEM showed that as the charge density increases Co particles get bigger and become like a thin film on the PPy surface. From EDX spectra, C, N, F peaks arising from the doped PPy layer, and Co peaks of the particles are seen clearly. The composite films having Co electrodeposited at the charge density lower than 600 mC cm^{-2} have a diamagnetic effect. The composite films with Co charge density of 600, 700, 4000 and 5000 mC cm^{-2} have isotropic behavior. Other films have anisotropic effects. The weak crystallization and the preferred orientation induce isotropic behavior.

ACKNOWLEDGEMENTS

This work was supported by Uludag University under Grant No. UAP(F)-2010/56 and AYP (F)-2015/8

REFERENCES

Cao Y, Wang Q, Li G, Du J, Wu C, He J, 2013. Effects of high magnetic field on the structure evolution, magnetic and electrical properties of the molecular beam vapor deposited Fe_xNi_{1-x} ($0.3<x<0.8$) thin films. Journal of Magnetism and Magnetic Materials 332: 38–43.

Chipara M, Skomski R, Sellmyer DJ, 2007. Electrodeposition and magnetic properties of polypyrrole–Fe nanocomposites. Material Letters 61: 2412–2415.

Chowdhury AN, Islam MS, Azam MS, 2007. Polyaniline matrix containing nickel ferromagnet. Journal of Applied Polymer Science 103: 321–327.

Damian A, Omanovic S, 2006. Ni and Ni Mo hydrogen evolution electrocatalysts electrodeposited in a polyaniline matrix. Journal of Power Sources 158: 464–476.

Davidson RG, Turner TG, 1995. An IR spectroscopic study of the electrochemical reduction of polypyrrole doped with dodecylsulfate anion. Synthetic Metals 72: 121-128.

Garcia B, Lamzoudi A, Pillier F, Le HNT, Deslouis C, 2002. Oxide/polypyrrole composite films for corrosion protection of iron. Journal of Electrochemical Society 149: B560-B566.

Haciismailoglu M, 2015. Effects of the PPy layer thickness on Co–PPy composite films. Applied Surface Science 356: 817–826.

Haciismailoglu M, Haciismailoglu MC, Alper M,·Schwarzacher W, 2014. Electrodeposition and Characterization of Co Particles on Ultrathin Polypyrrole Films. Journal of Superconductivity and Novel Magnetism 27: 2599-2606.

Heinig NF, Kharbanda N, Pynenburg MR, Zhou XJ, Schultz GA, Leung KT, 2008. The growth of nickel nanoparticles on conductive polymer composite electrodes. Material Letters 62: 2285–2288.

Hepel M, Chen VM, Stephenson R, 1996. Effect of the composition of polypyrrole substrate on the electrodeposition of copper and nickel. Journal of Electrochemical Society143: 498-505.

Iannotti V, Ausanio G, Campana C, D'Orazio F, Hison C, Lucari F, Lanotte L, 2008. Magnetic anisotropy in Ni–Si nanoparticle films produced by ultrashort pulsed laser deposition. . Journal of Magnetism and Magnetic Materials 320: e594–e598.

Kato H, Nisbikawa O, Matsui T, Honma S, Kokados H, 1991. Fourier transform infrared spectroscopy study of conducting polymer polypyrrole: higher order structure of electrochemically synthesized film. Journal of Physical Chemistry 95: 6014-6016.

Kaur D, Chaudhary S, Pandya DK, Gupta R, Kotnala RK, 2013. Magnetization reversal studies in structurally tailored cobalt nanowires. . Journal of Magnetism and Magnetic Materials 344: 72–78.

Ko JM, Park DY, Myung NV, Chung JS, Nobe K, 2002. Electrodeposited conducting polymer–magnetic metal composite films. Synthetic Metals 128: 47–50.

Lee JY, Tan TC, 1990. Cyclic voltammetry of electrodeposition of metal on electrosynthesized polypyrrole film, . Journal of Electrochemical Society 137: 1402-1408.

Lei J, Liang W, Martin CR, 1992. Infrared investigations of pristine, doped and partially doped polypyrrole. Synthetic Metals 48: 301–312.

Liu YC, Hwang BJ, 1999. Interaction of copper(I)-polypyrrole complexes prepared by depositing-dissolving copper onto and from polypyrroles. Thin Solid Films 339: 233-239.

Martins dos Santos LM, Lacroix JC, Chane-Ching KI, Adenier A, Abrantes LM, Lacaze PC, 2006. Electrochemical synthesis of polypyrrole films on copper electrodes in acidic and neutral aqueous media. Journal of Electroanalytical Chemistry 587: 67–78.

McNally E, Zhitomirsky I, Wilkinson D, 2005. Cathodic electrodeposition of cobalt oxide films using polyelectrolytes. Materials Chemistry and Physics 91: 391-398.

Orinakova R, Filkusova M, 2010. Hydrogen evolution on microstructured polypyrrole films modified with nickel. Synthetic Metals 160: 927–931.

Street GB, Clarke TC, Krounbi M, Kanazawa K, Lee V, Pfluger P, Scott JC, Weiser G, 1982. Preparation and characterization of neutral and oxidized polypyyrole films. Molecular Crystals and Liquid Crystals 83: 253-264.

Tian B, Zerbi G, 1990. Lattice dynamics and vibrational spectra of polypyrrole. Journal of Chemical Physics 92: 3886-3891.

Tian L, Qi Y, Wang B, 2009. Electrochemical preparation and structural characterization of platinum thin film on a polypyrrole film modified ITO electrode. Journal of Colloid Interface Science 333: 249–253.

Torsi L, Pezzuto M, Siciliano P, Rella R, Sabbatini L, Valli L, Zambonin PG, 1998. Conducting polymers doped with metallic inclusions: New materials for gas sensors. Sensors and Actuators B 48: 362–367.

Trung T, Trung TH, Ha CS, 2005. Preparation and cyclic voltammetry studies on nickel-nanoclusters containing polyaniline composites having layer-by-layer structures. Electrochimica Acta 51: 984–990.

Tsakova V, 2008. How to affect number, size, and location of metal particles deposited in conducting polymer layers. Journal of Solid State Electrochemistry 12: 1421–1434.

Vassar A, Roncali J, Garnier F, 1988. Preparation and electroactivity of poly(thiophene) electrodes modified by electrodeposition of palladium particles. Journal of Electroanalytical Chemistry 255: 53-69.

Vork FTA, Janssen LJJ, Barendrechi E, 1986. Oxidation of hydrogen at platinum-polypyrrole electrodes, Electrochimica Acta 31:1569 -1575.

Watanabe N, Morais J, Accione SBB, Morrone A, Schmidt JE, Martins Alves MC, 2004. Electronic, Structural, and Magnetic Properties of Cobalt Aggregates Embedded in Polypyrrole. Journal of Physical Chemistry B 108: 4013-4017.

Zolopa MW, Gradzka E, Szymanski K, Winkler K, 2013. Electrodeposition of nickel, cobalt, and iron on polypyrrole films, Thin Solid Films 548: 44–51.